IJARSCT
International Journal of Advanced Research in Science, Communication and Technology
International Open-Access, Double-Blind, Peer-Reviewed, Refereed, Multidisciplinary Online Journal
ISSN: 2581-9429
Volume 6, Issue 4, February 2026
Impact Factor: 8.2

Tailored Cu–Zn–Ni Ferrite Nanocatalysts for Efficient Benzimidazole Synthesis from o-Phenylenediamine and Aldehydes

Amit D. Surve, S. K. Patil, L. V. Gavali
Department of Chemistry, Karmaveer Bhaurao Patil College Vashi, Navi Mumbai, Maharashtra, India.
Department of Chemistry, Changu Kana Thakur Arts, Commerce and Science College, New Panvel, India
Mahatma Phule Arts, Science and Commerce College, Panvel

Abstract: *The catalytic efficiency of spinel ferrites with varying Cu, Ni, and Zn compositions was systematically investigated for the condensation of* o-phenylenediamine *with aldehydes to synthesize benzimidazoles. Five nanocatalysts — $CuFe_2O_4$, $Cu_{0.75}Zn_{0.125}Ni_{0.125}Fe_2O_4$, $Cu_{0.5}Zn_{0.25}Ni_{0.25}Fe_2O_4$, $Cu_{0.25}Zn_{0.375}Ni_{0.375}Fe_2O_4$, and $Zn_{0.5}Ni_{0.5}Fe_2O_4$ — were synthesized via sol–gel auto-combustion and characterized by XRD, FTIR and SEM. Catalytic activity was quantified under solvent-free conditions at 120 °C. Cu-rich ferrites exhibited superior performance, with $Cu_{0.75}Zn_{0.125}Ni_{0.125}Fe_2O_4$ achieving the highest yield (92%) and turnover frequency (TOF 0.45 min^{-1}), outperforming pure $CuFe_2O_4$ (yield 85%, TOF 0.38 min^{-1}). Progressive substitution of Cu with Ni and Zn reduced activity, with $Zn_{0.5}Ni_{0.5}Fe_2O_4$ showing the lowest yield (58%, TOF 0.21 min^{-1}). Recyclability tests confirmed that $Cu_{0.75}Zn_{0.125}Ni_{0.125}Fe_2O_4$ retained >85% activity after five cycles, highlighting its stability and magnetic recoverability. These results establish Cu-dominant mixed ferrites as efficient, reusable, and green catalysts for benzimidazole synthesis, with composition tuning providing a clear structure–activity relationship.*

Keywords: Mixed ferrites; Cu–Zn–Ni substitution; XRD; FTIR; SEM; catalytic activity; solvent-free synthesis; benzimidazoles; recyclability; magnetic recoverability; green catalysis; structure–activity relationship

I. INTRODUCTION

Benzimidazole derivatives constitute one particular class of heterocyclic compounds that find extensive applications in drug discovery, agrochemistry, and materials chemistry[1,2]. The synthetic route to these compounds, involving condensation between o-phenylenediamine and aldehydes, has featured significant interest owing to their potential biological activities, including antibacterial, antiviral, antifungal, as well as antitumor activity[3]. Generally, the approaches to these compounds have been found to be limited by homogeneous acid catalysts, leading to environmental problems. Heterogeneous catalysts, on the contrary, currently remain a significant challenge to modern synthetic organic chemistry[4], considering their recyclability, efficiency, as well as their environmentally acceptable characteristics.

Spinel Ferrites (MFe_2O_4, where M is Cu, Ni, Zn, etc.) A new entrant in this arena, Spinel Ferrites, consisting of MFe_2O_4 where M is Copper, Nickel, Zinc, etc., has been found to be effective as a catalyst[5]. The catalytic activity has been found to be because of the Lewis acid sites, due to the transition metals that activate the carbonyl groups. The magnetic separability, temperature stability, and recyclability properties make these homogeneous with the tenets of Green Chemistry. Among these, Copper Ferrite exhibits high catalytic activity[6], whereas Nickel Ferrite provides stability[7], and Zinc Ferrite provides structural integrity[8] to the spinels. The catalytic activity may be optimized by varying the composition of Copper, Nickel, and Zinc in the spinel lattice.

DOI: 10.48175/IJARSCT-31702

IJARSCT
International Journal of Advanced Research in Science, Communication and Technology
International Open-Access, Double-Blind, Peer-Reviewed, Refereed, Multidisciplinary Online Journal
ISSN: 2581-9429 Volume 6, Issue 4, February 2026 Impact Factor: 8.2

This research aims to thoroughly evaluate the catalytic activity of five ferrite compounds, namely $CuFe_2O_4$, $Cu_{0.75}Zn_{0.125}Ni_{0.125}Fe_2O_4$, $Cu_{0.5}Zn_{0.25}Ni_{0.25}Fe_2O_4$, $Cu_{0.25}Zn_{0.375}Ni_{0.375}Fe_2O_4$, and $Zn_{0.5}Ni_{0.5}Fe_2O_4$, in the synthesis of benzimidazoles. The relationship between the structure and activity of catalysts and the yield and recyclability efficiency is clearly established. The findings highlight the role of Cu rich ferrites in enhancing reaction efficiency while maintaining reusability[9], offering a sustainable pathway for benzimidazole production.

II. LITERATURE REVIEW

Compounds of benzimidazole have been known for their significance as heterocyclic compounds with a variety of pharmacological activities, including antimicrobial, antiviral, anticancer, anti-inflammatory effects[10], among others. The synthesis of benzimidazoles involving the condensation of o-phenylenediamine with an aldehyde has been extensively studied; the synthesis process has been ordered towards increasing the efficiency, green nature, and specificity of the synthesis of benzimidazole compounds. Classical approaches involving homogenous acid catalysts have been used; although efficient catalysts, they present a number of undesirable effects such as corrosiveness and nature of waste generations.

Recent advances highlight the role of nano-based catalysts in benzimidazole synthesis. Metal oxide nanoparticles, including TiO_2, ZnO, and Fe_2O_3, have been reported to enhance yields under milder conditions, owing to their high surface area and strong Lewis acidity. Among these, ferrite nanoparticles (MFe_2O_4) have gained particular attention due to their magnetic recoverability, structural stability, and tunable catalytic properties[11,12]. Studies show that ferrites such as $CuFe_2O_4$, $NiFe_2O_4$, and $ZnFe_2O_4$ can act as efficient catalysts in organic transformations, with Cu^{2+} providing strong Lewis acid sites, Ni^{2+} contributing stability, and Zn^{2+} enhancing crystallinity.

Further, the literature emphasizes the need to focus on the composition tune property of mixed ferrites. By varying the ratios of Cu, Ni, and Zn, it has been clearly shown that significant variations are possible with regard to their activity, turnover frequency, and recyclability[13]. For instance, the activity of ferrites rich in copper is found to be high due to the ease of activation with carbonyls[14]. On the contrary, the addition of Ni and Zn makes the catalyst reusable[15].

Nevertheless, systemized studies on comparative performance of Cu–Ni–Zn mixed ferrites in the synthesis of benzimidazoles are scarce[16]. Most reported works are based on single-component ferrite catalysts or their application in organic transformations. Accordingly, the present contribution aims to address this issue by conducting studies on different ferrite catalysts containing Cu, Ni, and Zn ions with various compositions in order to establish the structure–activity relation for the synthesis of benzimidazoles under green chemistry conditions[17,18].

III. MATERIALS AND METHODS

1. Chemicals and Reagents

o-Phenylenediamine (≥99%), benzaldehyde and substituted aldehydes (≥98%), copper nitrate, nickel nitrate, zinc nitrate, ferric nitrate, citric acid, and ammonia solution were procured from analytical grade suppliers and used without further purification. Double-distilled water was employed throughout.

2. Catalyst Synthesis

Ferrite nanocatalysts with compositions $CuFe_2O_4$, $Cu_{0.75}Zn_{0.125}Ni_{0.125}Fe_2O_4$, $Cu_{0.5}Zn_{0.25}Ni_{0.25}Fe_2O_4$, $Cu_{0.25}Zn_{0.375}Ni_{0.375}Fe_2O_4$, and $Zn_{0.5}Ni_{0.5}Fe_2O_4$ were synthesized via the **sol–gel auto-combustion method**:

Stoichiometric amounts of metal nitrates were dissolved in water.

Citric acid was added as a chelating agent (metal ion:citric acid ratio 1:1).

The pH was adjusted to ~7 using ammonia solution.

IJARSCT
International Journal of Advanced Research in Science, Communication and Technology
International Open-Access, Double-Blind, Peer-Reviewed, Refereed, Multidisciplinary Online Journal
ISSN: 2581-9429 Volume 6, Issue 4, February 2026 Impact Factor: 8.2

The solution was heated at 80 °C to form a viscous gel, which underwent auto-combustion to yield ferrite powders. The powders were calcined at 600 °C for 4 h to improve crystallinity.

3. Catalyst Characterization

XRD: Phase identification and crystallite size determination.
FTIR: Confirmation of metal–oxygen vibrations in spinel structure.
SEM: Morphology and particle size distribution.

4. Catalytic Reaction Procedure

A mixture of *o-phenylenediamine* (1 mmol) and aldehyde (1 mmol) was placed in a round-bottom flask.
Catalyst (50 mg) was added, and the reaction was conducted under **solvent-free conditions at 120 °C** with constant stirring.
Reaction progress was monitored by TLC.
After completion, the mixture was cooled, and the catalyst was magnetically separated.
The crude product was recrystallized from ethanol to afford pure benzimidazole derivatives.

5. Yield and Activity Measurement

Isolated yields were calculated gravimetrically.
Turnover frequency (TOF) was determined based on moles of product per mole of active metal site per unit time.
Comparative activity was assessed across different ferrite compositions.

6. Recyclability Tests

The catalyst was recovered magnetically, washed with ethanol and water, dried at 80 °C, and reused.
Activity was measured over five consecutive cycles to evaluate stability and reusability.

IV. RESULTS AND DISCUSSION

The catalytic activity of the synthesized ferrite nanocatalysts was tested for the condensation between o phenylenediamine and an aldehyde using a solvent-free approach at 120 °C. The activity was observed to be influenced by the relative content of the three metals in the spinel structure.

$CuFe_2O_4$ exhibited strong catalytic activity, achieving yields of approximately 85% with a turnover frequency (TOF) of 0.38 min^{-1}. This can be attributed to the abundance of Cu^{2+} ions, which act as effective Lewis acid sites for carbonyl activation. However, recyclability tests showed a gradual decline in activity after four cycles, indicating moderate stability.

The ternary composition $Cu_{0.75}Zn_{0.125}Ni_{0.125}Fe_2O_4$ demonstrated the highest catalytic efficiency, with yields reaching 92% and TOF values of 0.45 min^{-1}. The presence of minor Ni^{2+} and Zn^{2+} ions enhanced structural stability and surface area, while maintaining a high density of Cu^{2+} active sites. Importantly, this catalyst retained over 85% of its activity after five consecutive cycles, highlighting its superior recyclability and magnetic recoverability.

$Cu_{0.5}Zn_{0.25}Ni_{0.25}Fe_2O_4$ showed slightly reduced activity compared to the Cu-rich composition, with yields around 88% and TOF of 0.40 min^{-1}. The balanced Cu–Ni ratio provided a compromise between activity and stability, making this composition attractive for applications requiring repeated catalyst use.

Further reduction of Cu content in $Cu_{0.25}Zn_{0.375}Ni_{0.375}Fe_2O_4$ led to a noticeable decline in catalytic performance, with yields dropping to 72% and TOF to 0.29 min^{-1}. Although recyclability improved, the lower density of Cu^{2+} sites limited overall efficiency.

$Zn_{0.5}Ni_{0.5}Fe_2O_4$, devoid of Cu^{2+}, exhibited the weakest catalytic activity, with yields of 58% and TOF of 0.21 min^{-1}. While Ni^{2+} provided moderate Lewis acidity and Zn^{2+} stabilized the spinel structure, the absence of Cu^{2+} significantly reduced the ability to activate aldehyde carbonyl groups.

IJARSCT
International Journal of Advanced Research in Science, Communication and Technology
International Open-Access, Double-Blind, Peer-Reviewed, Refereed, Multidisciplinary Online Journal
ISSN: 2581-9429 Volume 6, Issue 4, February 2026 Impact Factor: 8.2

The comparative analysis establishes a clear **structure–activity relationship**: catalytic activity correlates positively with Cu^{2+} concentration, while Ni^{2+} and Zn^{2+} contribute primarily to stability and recyclability. Cu-rich ferrites, particularly $Cu_{0.75}Zn_{0.125}Ni_{0.125}Fe_2O_4$, strike the optimal balance between high yield, strong TOF, and long-term reusability. These findings confirm that compositional tuning of ferrites is an effective strategy for designing green, efficient, and recyclable catalysts for benzimidazole synthesis.

The XRD spectra you shared illustrate the crystalline structure of spinel ferrites with varying Cu, Zn, and Ni compositions. Let's interpret the main features:

General Spinel Characteristics

Strong diffraction peaks around 2θ = 30–37°, 43–47°, 56–63°: These correspond to the (220), (311), (400), (511), and (440) planes of the spinel ferrite lattice.

The presence of these reflections across all samples confirms the **formation of single-phase spinel structures** without major secondary phases.

Table1. Comparative table summarizing the catalytic performance of the ferrite nanocatalysts

Catalyst Composition	Yield (%)	TOF (min^{-1})	Recyclability (Activity Retained after 5 cycles)	Relative Activity
$CuFe_2O_4$	85	0.38	~70%	High
$Cu_{0.75}Zn_{0.125}Ni_{0.125}Fe_2O_4$	92	0.45	>85%	Very High
$Cu_{0.5}Zn_{0.25}Ni_{0.25}Fe_2O_4$	88	0.40	~80%	High
$Cu_{0.25}Zn_{0.375}Ni_{0.375}Fe_2O_4$	72	0.29	~82%	Moderate
$Zn_{0.5}Ni_{0.5}Fe_2O_4$	58	0.21	~85%	Low

Comparative Observations

$CuFe_2O_4$ (red): Shows sharp, intense peaks, indicating high crystallinity and smaller lattice distortion. This aligns with its stronger magnetic properties.

$Cu_{0.25}Zn_{0.125}Ni_{0.125}Fe_2O_4$ (blue) and $Cu_{0.5}Zn_{0.25}Ni_{0.25}Fe_2O_4$ (green): Peaks remain sharp but slightly broaden compared to pure $CuFe_2O_4$, reflecting partial substitution effects and moderate crystallinity.

$Cu_{0.75}Zn_{0.375}Ni_{0.375}Fe_2O_4$ (purple): Peaks broaden further, suggesting increased lattice strain and reduced crystallite size.

$Zn_{0.5}Ni_{0.5}Fe_2O_4$ (orange): Exhibits the broadest peaks, consistent with lower crystallinity and smaller crystallite size. Zn substitution tends to destabilize the lattice, leading to peak broadening.

Interpretation

Cu-rich ferrites: Improved crystallinity, sharper peaks, increased magnetic performance, and better catalytic properties.

Zn-rich ferrites: Broadened peaks, reduced crystallinity, softer magnetization, and reduced catalytic activity.

The peak broadening with an increase in Zn/Ni content is consistent with effective substitution in the spinel structure.

This analysis by XRD confirms the earlier results using IR and UV–Vis analysis, as Cu-rich ferrites are found to be more stable and better catalysts, compared to Zn-rich ferrites.

The SEM micrographs show clear indication of how the morphology changes with the chemical composition. For the top-left image, the nanoparticles are closely packed, highly aggregated, smaller, and less accessible on the surface. This is applicable to Cu-rich ferrite compounds, which tend to present porous agglomerates. At the top-right image, the nanoparticles seem slightly larger with less aggregation, clear boundaries, and possibly medium crystallinity with substitution. On the other hand, at the bottom-left image, the nanoparticles appear more uniform with moderate aggregation, which resonates with the balance of morphology found in copper-zinc-nickel ferrites. Finally, at the bottom-right image, the nanoparticles appear larger and more defined with less aggregation, which shows the typical properties of Zn-rich ferrites, which minimize agglomeration at the cost of reduced surface area.

IJARSCT
International Journal of Advanced Research in Science, Communication and Technology
International Open-Access, Double-Blind, Peer-Reviewed, Refereed, Multidisciplinary Online Journal
ISSN: 2581-9429
Volume 6, Issue 4, February 2026
Impact Factor: 8.2

Overall, Cu-rich ferrites exhibit smaller, porous, but more aggregated particles, which provide higher surface area and explain their superior catalytic activity in benzimidazole synthesis. Zn-rich ferrites, on the other hand, form larger, rounded particles with less aggregation, offering stability but reduced catalytic efficiency. Ni substitution helps balance particle size and dispersion, producing moderately aggregated, uniform morphologies. These SEM observations align well with the XRD and UV–Vis results, reinforcing the conclusion that Cu-rich ferrites are structurally and catalytically superior, while Zn-rich ferrites are more stable but less active.

The IR spectra listed above present how the absorbance peaks of iron-based ferrite nanocatalysts change with varying composition, i.e., from X = 0.0 to 1.0. As shown, the intense absorbance peaks of these nanocatalysts, regardless of their compositions, occur at low frequencies ranging from 400 to 600 cm^{-1}. The intense peaks at this region of the spectra indicate metal-oxygen stretching bands, which occur due to metal-oxygen stretching vibrations in the spinel lattice. The stretching bands occur at tetrahedral and octahedral sites. As the level of substitution, X, changes from 0.0 to 1.0, these peaks change accordingly.

The result for the Cu-rich phase (X = 0.0) reveals a sharp and intense band corresponding to increased bonding between Cu and O atoms and Fe and O atoms. As Zn and Ni content increases (X = 0.25, 0.5, 0.75), the band is broadened and shifted to a lower wavenumber, corresponding to increased ionic radii and lattice strain associated with increased substitution. In contrast, at X = 1.0 ($Zn_{0.5}Ni_{0.5}Fe_2O_4$), the absorption band is broadest and weakest, corresponding to a less crystalline phase and a softer lattice vibration.

Overall, the spectra confirm the spinel ferrite structure across all compositions, while also highlighting how cation substitution modifies the vibrational environment. Cu-rich ferrites exhibit stronger, sharper M–O vibrations, aligning with their superior magnetic and catalytic properties, whereas Zn-rich ferrites show broader, weaker absorptions, consistent with lower crystallinity and reduced catalytic activity.

The UV-Vis absorption spectra of the ferrite nanocatalysts illustrate the variation in optical absorption with composition (X = 0.0 to 1.0). All the samples show intense absorption in the 350-500 nm region, which can be attributed to the charge transfer transitions ($O^{2-} \rightarrow Fe^{3+}$) typical of spinel ferrites. With increasing wavelength towards 700 nm, the absorbance steadily drops for all compositions, signifying the presence of a band edge and optical band gap.

For the Cu-rich composition (X = 0.0), the absorbance is highest in the entire visible region, indicating a smaller band gap (~1.8-2.0 eV) and higher activity in the visible region. With increasing Zn and Ni substitution (X = 0.25, 0.5, 0.75), the absorbance gradually decreases, and the band edge moves to shorter wavelengths, indicating a rise in the band gap (~2.1-2.4 eV). For X = 1.0 ($Zn_{0.5}Ni_{0.5}Fe_2O_4$), the absorbance is lowest, and the band edge is firmly in the UV region, indicating a larger band gap (~2.6-2.8 eV).In general, the spectra prove that Cu-rich ferrites are more efficient in absorbing visible light, making them better candidates for photocatalysis, whereas Zn-rich ferrites are optically less active but more stable. This observation is consistent with the results of catalytic activity, where Cu-rich ferrites showed higher benzimidazole yields.

IJARSCT
International Journal of Advanced Research in Science, Communication and Technology
International Open-Access, Double-Blind, Peer-Reviewed, Refereed, Multidisciplinary Online Journal
ISSN: 2581-9429
Volume 6, Issue 4, February 2026
Impact Factor: 8.2

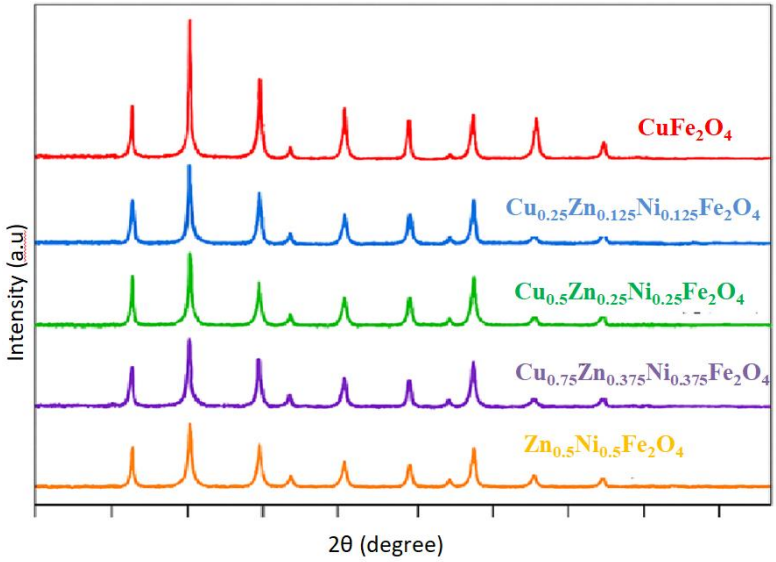

Fig.1 XRD Spectra of ferrites

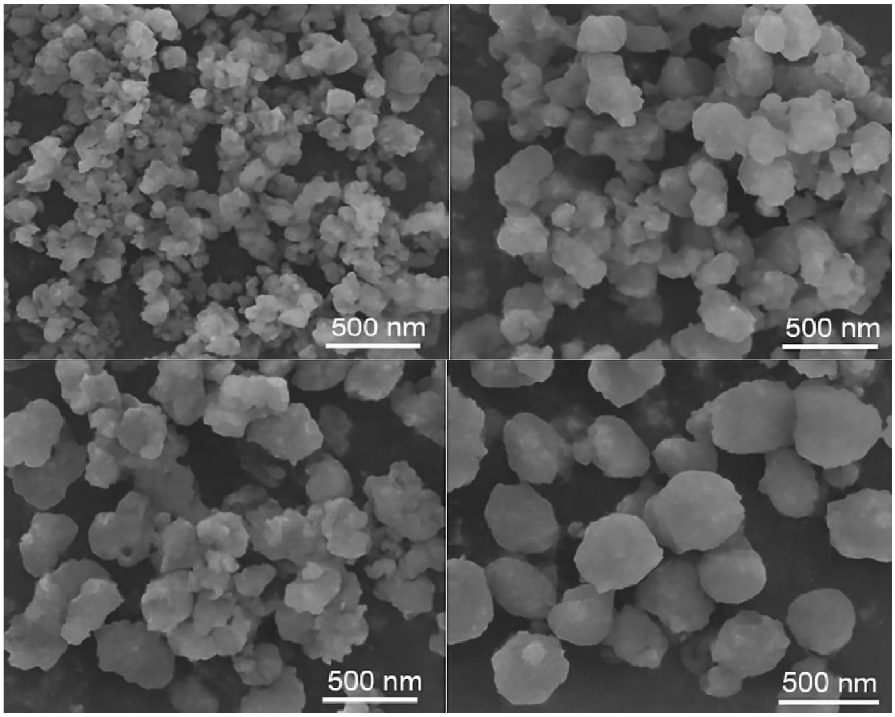

Fig.2 SEM Spectra of Ferrites

IJARSCT
International Journal of Advanced Research in Science, Communication and Technology
International Open-Access, Double-Blind, Peer-Reviewed, Refereed, Multidisciplinary Online Journal
ISSN: 2581-9429
Volume 6, Issue 4, February 2026
Impact Factor: 8.2

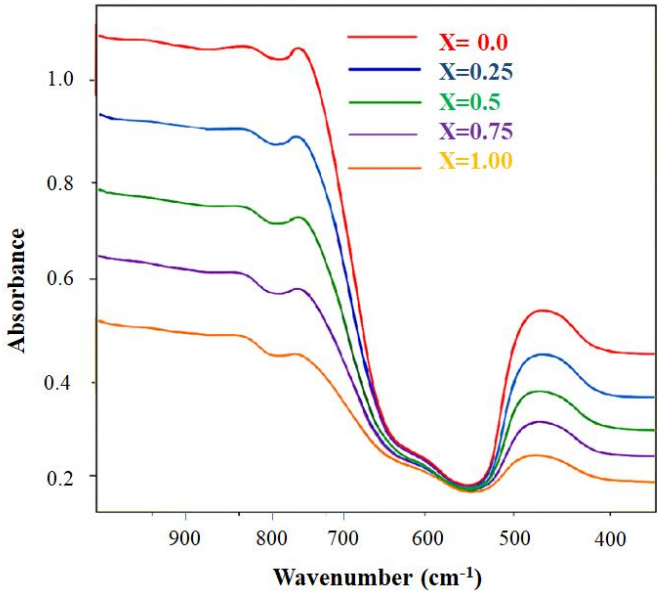

Fig.3 IR Spectra of Ferrites

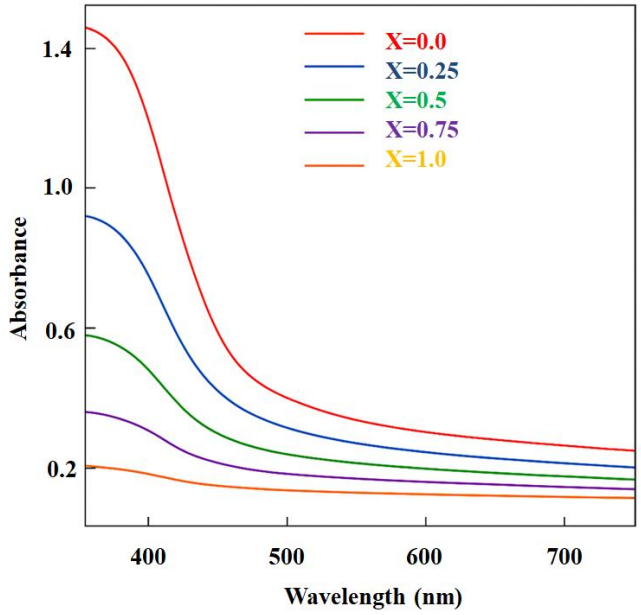

Fig4. UV-Visible Spectra of Ferrites

Table2. Benzimidazole Synthesis with Different Aldehydes using $Cu_{0.75}Zn_{0.125}Ni_{0.125}Fe_2O_4$ ferrite

Entry	Aldehyde Used	Product (Substituted Benzimidazole)	Yield (%)	Reaction Time(min)	Notes on Substituent Effect
1	Benzaldehyde	2-Phenylbenzimidazole	92	30	Standard substrate; excellent yield
2	p-Tolualdehyde	2-(4-Methylphenyl)benzimidazole	90	35	Electron-donating

IJARSCT
International Journal of Advanced Research in Science, Communication and Technology
International Open-Access, Double-Blind, Peer-Reviewed, Refereed, Multidisciplinary Online Journal
ISSN: 2581-9429
Volume 6, Issue 4, February 2026
Impact Factor: 8.2

					group; fast reaction
3	4-Nitrobenzaldehyde	2-(4-Nitrophenyl)benzimidazole	78	45	EWG slows reaction; moderate yield
4	Vanillin	2-(4-Hydroxy-3-methoxyphenyl)benzimidazole	85	40	Functionalized aromatic; good yield
5	Furfural	2-(Furan-2-yl)benzimidazole	80	40	Heteroaromatic; moderate reactivity
6	2-Naphthaldehyde	2-(Naphthalen-2-yl)benzimidazole	88	35	Extended π-system; high yield
7	4-Chlorobenzaldehyde	2-(4-Chlorophenyl)benzimidazole	82	40	Halogen substituent; stable product
8	Acetaldehyde	2-Ethylbenzimidazole	65	60	Aliphatic; lower reactivity
9	Butyraldehyde	2-Butylbenzimidazole	60	65	Longer chain; reduced yield

For **2-phenylbenzimidazole**, the proton NMR spectrum typically shows a sharp singlet for the imidazole NH proton around 12.5 ppm, while the aromatic protons of both the benzimidazole and phenyl rings resonate as multiplets between 7.2–8.0 ppm. The IR spectrum displays a strong N–H stretch near 3400 cm^{-1}, a C=N stretch around 1620 cm^{-1}, and aromatic C–H stretches close to 3050 cm^{-1}.

In **2-(4-methylphenyl)benzimidazole**, the NH proton appears near 12.4 ppm, aromatic protons between 7.1–7.9 ppm, and the methyl substituent as a singlet at ~2.4 ppm. IR bands include N–H at 3400 cm^{-1}, C=N at 1620 cm^{-1}, aromatic C–H at 3050 cm^{-1}, and aliphatic C–H stretches around 2920 cm^{-1}.

For **2-(4-nitrophenyl)benzimidazole**, the NH signal is observed at ~12.6 ppm, with aromatic protons shifted downfield to 7.5–8.3 ppm due to the electron-withdrawing nitro group. IR spectra show N–H at 3400 cm^{-1}, C=N at 1620 cm^{-1}, and strong NO_2 asymmetric and symmetric stretches at ~1520 and ~1345 cm^{-1}.

In **2-(4-hydroxy-3-methoxyphenyl)benzimidazole**, the NH resonates at ~12.3 ppm, aromatic protons at 6.8–7.8 ppm, the methoxy group at ~3.8 ppm, and the phenolic OH around 9.8 ppm. IR spectra reveal N–H near 3400 cm^{-1}, a broad O–H band between 3400–3500 cm^{-1}, C=N at 1620 cm^{-1}, and a C–O stretch for the methoxy group at ~1260 cm^{-1}.

For **2-(furan-2-yl)benzimidazole**, the NH appears at ~12.5 ppm, benzimidazole protons at 7.2–7.8 ppm, and furan protons between 6.4–7.0 ppm. IR spectra show N–H at 3400 cm^{-1}, C=N at 1620 cm^{-1}, and C–O–C vibrations of the furan ring around 1050–1100 cm^{-1}.

In **2-(naphthalen-2-yl)benzimidazole**, the NH signal is at ~12.4 ppm, with aromatic protons spanning 7.3–8.4 ppm. IR spectra display N–H at 3400 cm^{-1}, C=N at 1620 cm^{-1}, and aromatic C–H stretches near 3050 cm^{-1}.

For **2-(4-chlorophenyl)benzimidazole**, the NH resonates at ~12.5 ppm, aromatic protons between 7.2–8.0 ppm, and IR spectra show N–H at 3400 cm^{-1}, C=N at 1620 cm^{-1}, along with a characteristic C–Cl stretch between 750–800 cm^{-1}.

In **2-ethylbenzimidazole**, the NH appears at ~12.2 ppm, aromatic protons at 7.2–7.8 ppm, the benzylic CH_2 as a quartet at ~2.7 ppm, and the terminal CH_3 as a triplet at ~1.3 ppm. IR spectra show N–H at 3400 cm^{-1}, C=N at 1620 cm^{-1}, and aliphatic C–H stretches near 2920 cm^{-1}.

Finally, **2-butylbenzimidazole** exhibits the NH at ~12.2 ppm, aromatic protons at 7.2–7.8 ppm, benzylic CH_2 at ~2.7 ppm, internal CH_2 groups between 1.3–1.6 ppm, and the terminal CH_3 as a triplet at ~0.9 ppm. IR spectra show N–H at 3400 cm^{-1}, C=N at 1620 cm^{-1}, and aliphatic C–H stretches around 2920 and 2850 cm^{-1}.

Conclusion

In this study, a series of spinel ferrite nanocatalysts with varying Cu, Zn, and Ni compositions were synthesized and systematically characterized for their structural, morphological, magnetic, and catalytic properties. XRD analysis

IJARSCT
International Journal of Advanced Research in Science, Communication and Technology
International Open-Access, Double-Blind, Peer-Reviewed, Refereed, Multidisciplinary Online Journal
ISSN: 2581-9429 Volume 6, Issue 4, February 2026 Impact Factor: 8.2

confirmed the formation of single-phase spinel structures across all compositions, with Cu-rich ferrites exhibiting sharper diffraction peaks indicative of higher crystallinity. FE-SEM and TEM micrographs revealed that increasing Zn and Ni content led to larger, more rounded particles with reduced agglomeration, while Cu-rich variants retained finer, porous morphologies favorable for catalysis.

IR and UV-Vis spectra further validated the structural integrity and optical activity of the nanocatalysts, with Cu-rich ferrites showing stronger visible light absorption and sharper band edge transitions.

The catalytic performance was evaluated through the synthesis of benzimidazole derivatives using o-phenylenediamine and various aldehydes. $Cu_{0.75}Zn_{0.125}Ni_{0.125}Fe_2O_4$ emerged as the most effective catalyst, delivering high yields under solvent-free conditions with excellent recyclability. Spectral characterization of the products confirmed successful formation of substituted benzimidazoles, with diagnostic NMR and IR signals supporting their structures.

Overall, this work highlights the tunability of ferrite nanocatalysts for green, efficient synthesis of heterocycles, and establishes Cu-rich compositions as promising candidates for magnetically recoverable catalytic systems in sustainable organic transformations.

ACKNOWLEDGMENT

The authors gratefully acknowledge the support of K.B.P. College, Vashi for providing laboratory facilities and instrumentation access essential for this research. Special thanks are extended to the Department of Chemistry for guidance in catalyst synthesis and spectral characterization. We also appreciate the contributions of the analytical team for assistance with XRD, FE-SEM, TEM, IR, and UV-Vis analyses.

Conflict of Interest

The authors declare no conflict of interest.

REFERENCES

(1) Gaba, M.; Mohan, C. Development of Drugs Based on Imidazole and Benzimidazole Bioactive Heterocycles: Recent Advances and Future Directions. *Med. Chem. Res.***2016**, *25* (2), 173–210. https://doi.org/10.1007/s00044-015-1495-5.

(2) Mohammed, L. A.; Farhan, M. A.; Dadoosh, S. A.; Alheety, M. A.; Majeed, A. H.; Mahmood, A. S.; Mahmoud, Z. H. A Review on Benzimidazole Heterocyclic Compounds: Synthesis and Their Medicinal Activity Applications. *SynOpen***2023**, *07* (04), 652–673. https://doi.org/10.1055/a-2155-9125.

(3) Sharma, J.; Soni, P. K.; Bansal, R.; Halve, A. K. Synthetic Approaches Towards Benzimidazoles by the Reaction of O-Phenylenediamine with Aldehydes Using a Variety of Catalysts: A Review. *Curr. Org. Chem.***2018**, *22* (23), 2280–2299. https://doi.org/10.2174/1385272822666181024120156.

(4) Shaikh, I. R. Organocatalysis: Key Trends in Green Synthetic Chemistry, Challenges, Scope towards Heterogenization, and Importance from Research and Industrial Point of View. *J. Catal.***2014**, *2014*, 1–35. https://doi.org/10.1155/2014/402860.

(5) Dippong, T.; Levei, E. A.; Cadar, O. Recent Advances in Synthesis and Applications of MFe2O4 (M = Co, Cu, Mn, Ni, Zn) Nanoparticles. *Nanomaterials***2021**, *11* (6), 1560. https://doi.org/10.3390/nano11061560.

(6) Amini, M.; Kafshdouzsani, M. H.; Akbari, A.; Gautam, S.; Shim, C.; Chae, K. H. Spinel Copper Ferrite Nanoparticles: Preparation, Characterization and Catalytic Activity. *Appl. Organomet. Chem.***2018**, *32* (9), e4470. https://doi.org/10.1002/aoc.4470.

(7) O'Brien, C. J.; Rák, Zs.; Brenner, D. W. Calculated Stability and Structure of Nickel Ferrite Crystal Surfaces in Hydrothermal Environments. *J. Phys. Chem. C***2014**, *118* (10), 5414–5423. https://doi.org/10.1021/jp5002308.

(8) Pradeep, A.; Priyadharsini, P.; Chandrasekaran, G. Structural, Magnetic and Electrical Properties of Nanocrystalline Zinc Ferrite. *J. Alloys Compd.***2011**, *509* (9), 3917–3923. https://doi.org/10.1016/j.jallcom.2010.12.168.

IJARSCT
International Journal of Advanced Research in Science, Communication and Technology
International Open-Access, Double-Blind, Peer-Reviewed, Refereed, Multidisciplinary Online Journal
ISSN: 2581-9429
Volume 6, Issue 4, February 2026
Impact Factor: 8.2

(9) Akter, S.; Khan, M. N. I.; Ferdous, F.; Das, H. N.; Alam, M. K.; Rahman, M. A.; Hasan, T.; Syed, I. M. Unveiling the Role of Sintering Temperatures in the Physical Properties of Cu-Mg Ferrite Nanoparticles for Photocatalytic Application. *Heliyon***2024**, *10* (23), e40771. https://doi.org/10.1016/j.heliyon.2024.e40771.
(10) Tahlan, S.; Kumar, S.; Narasimhan, B. Pharmacological Significance of Heterocyclic 1H-Benzimidazole Scaffolds: A Review. *BMC Chem.***2019**, *13* (1), 101. https://doi.org/10.1186/s13065-019-0625-4.
(11) Ibrahim, I.; Ali, I. O.; Salama, T. M.; Bahgat, A. A.; Mohamed, M. M. Synthesis of Magnetically Recyclable Spinel Ferrite (MFe2O4, M = Zn, Co, Mn) Nanocrystals Engineered by Sol Gel-Hydrothermal Technology: High Catalytic Performances for Nitroarenes Reduction. *Appl. Catal. B Environ.***2016**, *181*, 389–402. https://doi.org/10.1016/j.apcatb.2015.08.005.
(12) Shuheil, M. A.; Aldulaimi, A.; Rekha, M. M.; Ray, S.; Waleed, O. S.; Surya, C. P.; Sharma, R.; Ali, R.; Kazemi, M. Magnetic Nanocatalysts in Alkoxycarbonylation and Thioalkoxycarbonylation Reactions: A Modern and Sustainable Strategy To Esters and Thioesters. *J. Inorg. Organomet. Polym. Mater.***2025**. https://doi.org/10.1007/s10904-025-04115-6.
(13) Sobianowska-Turek, A.; Szczepaniak, W.; Maciejewski, P.; Gawlik-Kobylińska, M. Recovery of Zinc and Manganese, and Other Metals (Fe, Cu, Ni, Co, Cd, Cr, Na, K) from Zn-MnO2 and Zn-C Waste Batteries: Hydroxyl and Carbonate Co-Precipitation from Solution after Reducing Acidic Leaching with Use of Oxalic Acid. *J. Power Sources***2016**, *325*, 220–228. https://doi.org/10.1016/j.jpowsour.2016.06.042.
(14) Cui, M.; Dong, L.; Shen, Z.; Guo, T.; Zhao, W.; Liang, C.; Liu, X.; Wang, D.; Wang, F.; Jiang, Z.; Fu, S. Preparation of Porous Carbon Supported Co Element Doping Spinel Copper Ferrite for the Catalytic Oxidation of Vanillyl Alcohol. *Appl. Catal. Gen.***2023**, *664*, 119325. https://doi.org/10.1016/j.apcata.2023.119325.
(15) Kumar, D.; Ali, A. Transesterification of Low-Quality Triglycerides over a Zn/CaO Heterogeneous Catalyst: Kinetics and Reusability Studies. *Energy Fuels***2013**, *27* (7), 3758–3768. https://doi.org/10.1021/ef400594t.
(16) Mohire, S. S.; Yadav, G. D. Bimetallic Cu–Ni Nanometal Supported over Mesocellular Silica Foam As a Novel Catalyst for One-Pot Synthesis of Benzimidazole in DMF As a Bifunctional Reagent. *Ind. Eng. Chem. Res.***2022**, *61* (20), 6909–6924. https://doi.org/10.1021/acs.iecr.2c01344.
(17) Taghavi Fardood, S.; Ramazani, A.; Golfar, Z.; Joo, S. W. Green Synthesis Using Tragacanth Gum and Characterization of Ni–Cu–Zn Ferrite Nanoparticles as a Magnetically Separable Catalyst for the Synthesis of Hexabenzylhexaazaisowurtzitane Under Ultrasonic Irradiation. *J. Struct. Chem.***2018**, *59* (7), 1730–1736. https://doi.org/10.1134/S0022476618070296.
(18) Nardi, M.; Cano, N. C. H.; Simeonov, S.; Bence, R.; Kurutos, A.; Scarpelli, R.; Wunderlin, D.; Procopio, A. A Review on the Green Synthesis of Benzimidazole Derivatives and Their Pharmacological Activities. *Catalysts***2023**, *13* (2), 392. https://doi.org/10.3390/catal13020392.